Zirconium and Hafnium Polyhydrides. Preparation and Characterization of $M_2H_3(BH_4)_5(PMe_3)_2$, $MH(BH_4)_3(dmpe)$, and $MH_2(BH_4)_2(dmpe)_2$

John E. Gozum and Gregory S. Girolami*

Contribution from the School of Chemical Sciences, The University of Illinois, Urbana-Champaign, 505 South Mathews Avenue, Urbana, Illinois 61801.
Received November 30, 1989. Revised Manuscript Received January 8, 1991

Abstract: Treatment of the zirconium and hafnium tetrahydroborate complexes $M(BH_4)_4$ with trimethylphosphine yields amber (M = Zr) or colorless (M = Hf) crystals of the new polyhydride complexes $Zr_2H_3(BH_4)_5(PMe_3)_2$ and $Hf_2H_3(BH_4)_5(PMe_3)_2$. These d^0 complexes exhibit triplets ($J_{PH} \approx 13$ Hz) for the hydride ligands in their ^1H NMR spectra at δ 3.96 (Zr) and 8.53 (Hf). The ^1H, $^{11}B\{^1H\}$, and $^{31}P\{^1H\}$ NMR spectra show that there is only one phosphine environment but two BH_4^- environments in a 2:3 ratio. Single-crystal X-ray diffraction studies of the two complexes in each case reveal a distinctly asymmetric dinuclear structure bridged by three hydrogen atoms. One metal center is ligated by three terminal tridentate BH_4^- groups, while the other is ligated by the two phosphines and by one tridentate and one bidentate BH_4^- group. All the metal-ligand distances in the zirconium complex are slightly longer than those in the hafnium complex, as expected from the relative ionic radii: Zr···Zr = 3.124 (1) Å, Zr-H_b = 1.92 (4) Å, Zr-P = 2.750 (1) Å, Zr-B = 2.346 (8) Å (η^3-BH_4), Zr-B = 2.604 (8) Å (η^2-BH_4), Zr-H-Zr = 109 (3)°; Hf···Hf = 3.076 (1) Å, Hf-P = 2.725 (6) Å, Hf-B = 2.34 (3) Å (η^3-BH_4), and Hf-B = 2.53 (3) Å (η^2-BH_4). Treatment of the $M(BH_4)_4$ complexes with the bidentate phosphine 1,2-bis(dimethylphosphino)ethane gives mononuclear hydrides of stoichiometry $MH(BH_4)_3(dmpe)$ or $MH_2(BH_4)_2(dmpe)_2$, depending on the conditions. The monohydride complexes $MH(BH_4)_3(dmpe)$ contain both bidentate and tridentate BH_4^- groups as judged by IR spectroscopy. The ^1H NMR spectra show a triplet for the terminal hydride groups at δ 6.08 (J_{PH} = 56 Hz) for M = Zr and 10.99 (J_{PH} = 45 Hz) for M = Hf. The ^1H NMR spectra also show that there are two PMe_2 environments, while the $^{11}B\{^1H\}$ and $^{31}P\{^1H\}$ NMR spectra show that there is a single BH_4^- and a single phosphorus environment. These data are consistent with a pseudooctahedral structure in which the three mutually *fac* BH_4^- groups are exchanging with each other. The BH_4^- groups in the dihydride complexes $MH_2(BH_4)_2(dmpe)_2$ are bidentate by IR spectroscopy. The ^1H NMR spectra show that there is one hydride environment and one BH_4^- environment but that the two ends of each dmpe ligand are inequivalent. The terminal hydride resonances at δ 3.38 (Zr) and 6.65 (Hf) are complex multiplets arising from the X part of XX'AA'BB' spin systems. Simulation of the resonances suggests that the coupling constant between the two hydride ligands may be unusually large at ca. 30 Hz. The possibility that nuclear exchange processes are responsible for this large coupling constant was ruled out on the basis of deuteration studies. Interestingly, these $MH_2(BH_4)_2(dmpe)_2$ molecules are nonfluxional at room temperature, despite the high coordination numbers (8 or 10, depending on how the BH_4^- groups are counted). Variable-temperature NMR spectroscopy shows that the molecules undergo an intramolecular fluxional process with an activation energy of 15.6 kcal mol^{-1}; this value is unusually high for a molecule with such a high coordination number. Crystal data for $Zr_2C_6H_{41}B_5P_2$ at −75 °C are as follows: orthorhombic; $P2_12_12_1$; a = 10.921 (2) Å, b = 12.255 (3) Å, c = 16.524 (6) Å, V = 2212 (1) Å^3, Z = 4, R_f = 0.031, R_{wf} = 0.029 for 301 variables and 2821 data for which $I > 2.58\sigma(I)$. Crystal data for $Hf_2C_6H_{41}B_5P_2$ at −75 °C are as follows orthorhombic; $P2_12_12_1$; a = 10.860 (7) Å, b = 12.248 (7) Å, c = 16.490 (4) Å, V = 2193 (3) Å^3, Z = 4, R_f = 0.042, R_{wf} = 0.051 for 112 variables and 1634 data for which $I > 2.58\sigma(I)$.

Introduction

Polyhydrides of the early transition elements are extremely rare,[1] despite the interesting chemistry exhibited by polyhydride derivatives of other transition elements.[2-6] Polyhydrides of tungsten and iridium, among others, are able to activate saturated hydrocarbons both photolytically and thermally.[7-10] However, for the group 4 elements, the only polyhydrides known are $Cp_2^*MH_2$ complexes[11-13] and related dicyclopentadienyl analogues,[14,17] the oligomeric monocyclopentadienyl complexes $[Cp^*ZrH_2(BH_4)]_2$,[18] $Cp^*_2Zr_2H_3Cl_3(PMe_3)$,[19] and $[Cp^*HfH_2Cl]_4$,[20] the phosphinoamide complexes $Hf_2H_3(BH_4)_3(npp)_2$, and $Hf_2H_4(BH_4)_2(npp)_2$, where npp = N-$(SiMe_2CH_2PMe_2)_2$.[21,22] Heterobimetallic complexes that contain three bridging hydrides between Zr and Os,[23] Zr and Re,[24] or between Zr and Y[25] are also known. Several of these molecules

(1) Toogood, G. E.; Wallbridge, M. G. H. *Adv. Inorg. Chem. Radiochem.* **1982**, *25*, 267-340.
(2) Muetterties, E. L. *Transition Metal Hydrides*; Marcel Dekker: New York, 1967.
(3) Bau, R. *Transition Metal Hydrides*, Advances in Chemistry Series 167; American Chemical Society: Washington, DC, 1978.
(4) Kaesz, H. D.; Saillant, R. B. *Chem. Rev.* **1972**, *72*, 231-281.
(5) Hlatky, G. G.; Crabtree, R. H. *Coord. Chem. Rev.* **1985**, *65*, 1-48.
(6) For the present discussion, a polyhydride will be defined as a coordination complex that contains more than one hydride per metal center.
(7) Green, M. L. H.; Berry, M.; Couldwell, C.; Prout, K. *Nouv. J. Chim.* **1977**, *1*, 187-188.
(8) Crabtree, R. H. *Chem. Rev.* **1985**, *85*, 1-48.
(9) Bergman, R. G. *Science (Washington, D.C)* **1984**, *223*, 902-908.
(10) Janowicz, A. H.; Periana, R. A.; Buchanan, J. M.; Kovac, C. A.; Bergman, R. G. *Pure Appl. Chem.* **1984**, *56*, 13-23.
(11) Bercaw, J. E.; Marvich, R. H.; Bell, L. G.; Brintzinger, H. H. *J. Am. Chem. Soc.* **1972**, *94*, 1219-1238.
(12) Manriquez, J. M.; McAlister, D. R.; Sanner, R. D.; Bercaw, J. E. *J. Am. Chem. Soc.* **1978**, *100*, 2716-2724.
(13) Roddick, D. M.; Fryzuk, M. D.; Seidler, P. F.; Hillhouse, G. L.; Bercaw, J. E. *Organometallics* **1985**, *4*, 97-104.
(14) Wailes, P. C.; Weigold, H.; Bell, A. P. *J. Organomet. Chem.* **1972**, *43*, C29-C31.
(15) Jones, S. B.; Petersen, J. L. *Inorg. Chem.* **1981**, *20*, 2889-2894.
(16) Weigold, H.; Bell, A. P.; Willing, R. I. *J. Organomet. Chem.* **1974**, *73*, C23-C24.
(17) Couturier, S.; Tainturier, G.; Gautheron, B. *J. Organomet. Chem.* **1980**, *195*, 291-306.
(18) Wolczanski, P. T.; Bercaw, J. E. *Organometallics* **1982**, *1*, 793-799.
(19) van der Hende, J. R.; Hessen, B.; Meetsma, A.; Teuben, J. H. *Organometallics* **1990**, *9*, 537-539.
(20) Booij, M.; Blenkers, J.; Sinnema, J. C. M.; Meetsma, A.; van Bolhuis, F.; Teuben, J. H. *Organometallics* **1988**, *7*, 1029-1032.
(21) Fryzuk, M. D.; Rettig, S. J.; Westerhaus, A.; Williams, H. D. *Inorg. Chem.* **1985**, *24*, 4316-4325.
(22) In addition, group 4 trihydrides of stoichiometry $MH_3(dmpe)$ have been reported to form upon hydrogenation of the benzyl complexes M-$(CH_2Ph)_4$ in the presence of 1,2-bis(dimethylphosphino)ethane: Tebbe, F. N. U.S. Pat. 3933876, 1976.
(23) Bruno, J. W.; Huffman, J. C.; Green, M. A.; Caulton, K. G.; *J. Am. Chem. Soc.* **1984**, *106*, 8310-8312.
(24) Sartain, W. J.; Huffman, J. C.; Lundquist, E. G.; Streib, W. G.; Caulton, K. G. *J. Mol. Catal.* **1989**, *56*, 20-35.

0002-7863/91/1513-3829$02.50/0

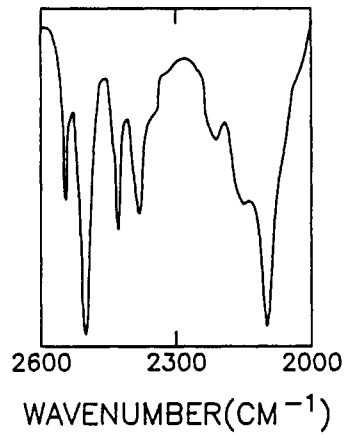

Figure 1. Infrared spectrum (Nujol mull) of $Zr_2H_3(BH_4)_5(PMe_3)_2$ (**1**) in the B–H stretching region. The spectrum of $Hf_2H_3(BH_4)_5(PMe_3)_2$ (**2**) is identical.

exhibit remarkable stoichiometric reactivities; for example, $Cp_2^*ZrH_2$ is able to convert carbon monoxide to methanol,[26] and other zirconium hydrides are able to promote the conversion of alkenes and alkynes to a variety of functionalized hydrocarbons.[27,28] In addition, transition-metal polyhydrides are potential precursors for the chemical vapor deposition of pure metals.

We have recently reported our synthetic approaches to polyhydrides of titanium or vanadium by treatment of titanium or vanadium poly(tetrahydroborates) with trialkylphosphines.[29-31] The binary zirconium and hafnium tetrahydroborate complexes $Zr(BH_4)_4$ and $Hf(BH_4)_4$ have long been known, but their reactions with Lewis bases have been little studied.[32] Recently, our research group and others have initiated studies in this area.[33,34] We now describe the preparation and characterization of new group 4 polyhydrides by addition of trialkylphosphines to $Zr(BH_4)_4$ or $Hf(BH_4)_4$. Both dinuclear products with bridging hydrides and mononuclear products with terminal hydrides are formed.

Results and Discussion

Reactions of $M(BH_4)_4$ with Unidentate Phosphines. The starting materials $Zr(BH_4)_4$ and $Hf(BH_4)_4$ are readily prepared by interaction of the appropriate tetrachloride with excess lithium tetrahydroborate in diethyl ether, followed by distillation of the product under vacuum.[35,36] Treatment of $M(BH_4)_4$ with excess trimethylphosphine in diethyl ether leads to the formation of an amber (Zr) or colorless (Hf) product, which may be crystallized from pentane. These new compounds possess the unusual stoichiometries $Zr_2H_3(BH_4)_5(PMe_3)_2$ (**1**) and $Hf_2H_3(BH_4)_5(PMe_3)_2$ (**2**) on the basis of spectroscopic and crystallographic data (Table I).

$$2M(BH_4)_4 + 5PMe_3 \rightarrow M_2H_3(BH_4)_5(PMe_3)_2 + 3BH_3{\cdot}PMe_3$$
$$\mathbf{1}: M = Zr \qquad \mathbf{2}: M = Hf$$

The infrared spectra of **1** and **2** show a number of bands in the B–H stretching region (Figure 1) and suggest that at least two

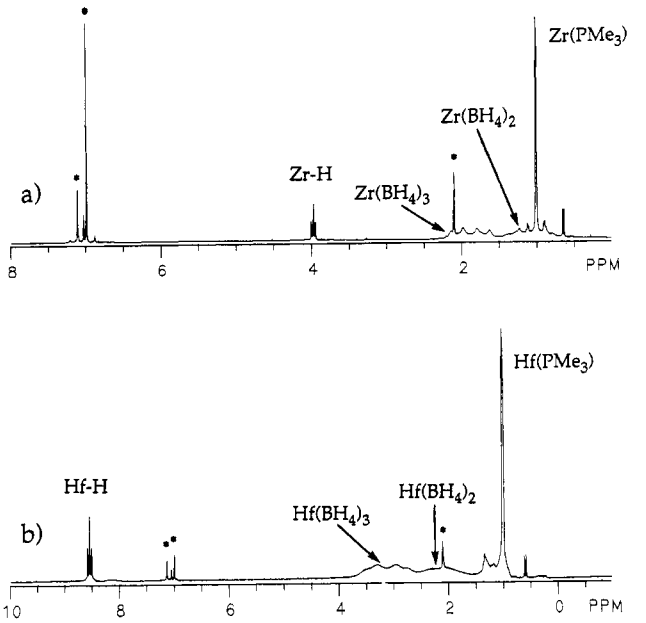

Figure 2. 300-MHz ^1H NMR spectra of (a) $Zr_2H_3(BH_4)_5(PMe_3)_2$ (**1**) and (b) $Hf_2H_3(BH_4)_5(PMe_3)_2$ (**2**) at 0 °C in C_7D_8. The small doublet at δ 0.80 is due to a trace of $PMe_3{\cdot}BH_3$. Solvent peaks are indicated with an asterisk.

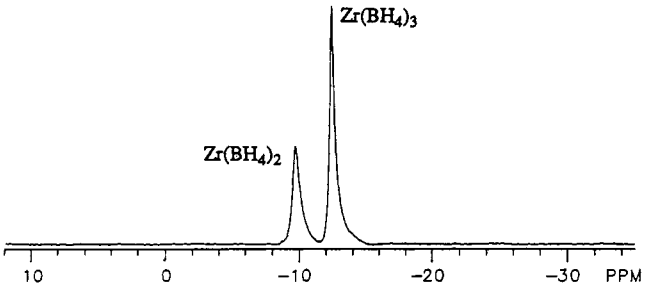

Figure 3. 96.3-MHz $^{11}B\{^1H\}$ NMR spectrum of $Zr_2H_3(BH_4)_5(PMe_3)_2$ (**1**) at 0 °C in C_7D_8. The spectrum of $Hf_2H_3(BH_4)_5(PMe_3)_2$ (**2**) is essentially identical.

BH_4^- coordination modes are present (e.g., bidentate and tridentate). The hydride ligands in these molecules bridge between the two metal centers (see below). We have been unable to identify which bands are due to M–H–M vibrational modes and which are due to low-frequency bending and wagging modes of the BH_4^- groups. Certainly, there are no absorptions in the 1500–2000-cm^{-1} region that are usually characteristic of terminal MH units.

The ^1H NMR spectra of **1** and **2** at 0 °C contain a virtually coupled triplet for the PMe_3 groups, two 1:1:1:1 quartets of relative intensity 3:2 for the BH_4^- groups, and a hydride resonance (Figure 2). The hydride signal appears at δ 3.96 for **1** and 8.53 for **2**, and both signals are triplets due to coupling with phosphorus ($^2J_{PH} \approx 13$ Hz). Above 0 °C, the hydride and PMe_3 resonances of the hafnium complex lose their triplet structure, evidently due to reversible phosphine dissociation. At −80 °C, the BH_4^- resonances broaden due to quadrupolar relaxation,[37] while the hydride and PMe_3 peaks remain sharp triplets.

The chemical shifts of tetravalent group 4 polyhydrides have been collected in Table II, and they illustrate the previously noted trend that resonances for terminal hydrides generally appear downfield of resonances for bridging hydrides.[15] Although the chemical shifts of both **1** and **2** fall in the terminal M–H range, there are a few zirconium and hafnium compounds with bridging hydrides that have chemical shifts near δ 4 and 8, respectively. Apparently, the polyhydrides of stoichiometry $[Cp_2MH_2]_2$ and their derivatives have hydride chemical shifts that are not representative of group 4 polyhydrides in general. In fact, both **1**

(25) Evans, W. J.; Meadows, J. H.; Hanusa, T. P. *J. Am. Chem. Soc.* **1984**, *106*, 4454–4460.
(26) Wolczanski, P. T.; Bercaw, J. E. *Acc. Chem. Res.* **1980**, *13*, 121–127.
(27) Wailes, P. C.; Weigold, H.; Bell, A. P. *J. Organomet. Chem.* **1972**, *43*, C32–C34.
(28) Schwartz, J.; Labinger, J. A. *Angew. Chem., Int. Ed. Engl.* **1976**, *15*, 333–340.
(29) Jensen, J. A.; Wilson, S. R.; Girolami, G. S. *J. Am. Chem. Soc.* **1988**, *110*, 4977–4982.
(30) Jensen, J. A.; Girolami, G. S. *Inorg. Chem.* **1989**, *28*, 2107–2113.
(31) Jensen, J. A.; Girolami, G. S. *Inorg. Chem.* **1989**, *28*, 2114–2119.
(32) Kravchenko, O. V.; Kravchenko, S. E.; Polyakova, V. B.; Makhaev, V. D.; Borisov, A. P.; Semenenko, K. H. *Koord. Khim.* **1982**, *8*, 1650–1654.
(33) Gozum, J. E.; Girolami, G. S. 198th American Chemical Society National Meeting, Miami, Florida, 1989, INOR 178.
(34) Baker, R. T.; Tebbe, F. N.; Calabrese, J. C. 198th American Chemical Society National Meeting, Miami, Florida, 1989, INOR 119.
(35) James, B. D.; Smith, B. E. *Synth. React. Inorg. Metal-Org. Chem.* **1974**, *4*, 461–465.
(36) James, B. D.; Nanda, R. K.; Wallbridge, M. G. H. *J. Chem. Soc. A* **1966**, 182–184.
(37) Marks, T. J.; Kolb, J. R. *Chem. Rev.* **1977**, *77*, 263.

Table I. NMR Data for the New Zirconium and Hafnium Polyhydride Complexes[a]

	$Zr_2H_3(BH_4)_5(PMe_3)_2$ (1)	$Hf_2H_3(BH_4)_5(PMe_3)_2$ (2)
	^1H NMR, 0 °C	
MH	3.96 (t, J_{PH} = 14)	8.53 (t, J_{PH} = 12)
$M(BH_4)_3$	1.87 (br q, J_{BH} = 86)	3.01 (br q, J_{BH} = 86)
$M(BH_4)_2$	1.05 (br q, J_{BH} = 88)	2.11 (br q, J_{BH} = 84)
$M(PMe_3)_2$	1.00 (t, J_{PH} = 3)	0.99 (t, J_{PH} = 4)
	$^{11}B\{^1H\}$ NMR, 0 °C	
$M(BH_4)_3$	−12.5 (s, fwhm = 65)	−14.5 (s, fwhm = 65)
$M(BH_4)_2$	−9.8 (s, fwhm = 90)	−12.1 (s, fwhm = 90)
	^{11}B NMR, 0 °C	
$M(BH_4)_3$	−12.5 (quintet, J_{BH} = 88)	−14.5 (quintet, J_{BH} = 86)
$M(BH_4)_2$	−9.8 (quintet, J_{BH} = 88)	−12.1 (quintet, J_{BH} = 86)
	$^{31}P\{^1H\}$ NMR, 0 °C	
$MPMe_3$	−21.2 (s)	−14.7 (s)
	$ZrH(BH_4)_3$(dmpe) (3)	$HfH(BH_4)_3$(dmpe) (4)
	^1H NMR, 20 °C	
MH	6.08 (t, J_{PH} = 56)	10.99 (t, J_{PH} = 45)
$M(BH_4)_3$	1.40 (br q, J_{BH} = 85)	2.65 (br q, J_{BH} = 88)
PMe_2	0.98 (d, J_{PH} = 8)	0.87 (d, J_{PH} = 8)
PMe_2	0.89 (d, J_{PH} = 7)	0.78 (d, J_{PH} = 7)
	^{11}B NMR, 20 °C	
$M(BH_4)_3$	−15.6 (quintet, J_{BH} = 87)	−15.7 (quintet, J_{BH} = 84)
	^{31}P NMR, 20 °C	
MP	0.2 (br d, J_{PH} = 53)	−3.8 (br d, J_{PH} = 41)
	$ZrH_2(BH_4)_2(dmpe)_2$ (5)	$HfH_2(BH_4)_2(dmpe)_2$ (6)
	^1H NMR, 25 °C	
MH	3.36 (m)[b]	6.65 (m)[c]
$M(BH_4)$	0.52 (q, J_{BH} = 80)	1.05 (q, J_{BH} = 84)
PMe_2	1.47 (d, J_{PH} = 5.5)	1.57 (d, J_{PH} = 5.5)
PMe_2	1.37 (br s)	1.47 (d, J_{PH} = 6.3)
PMe_2	1.37 (br s)	1.44 (br s)
PMe_2	1.30 (br s)	1.40 (br s)
PCH_2	1.55 (br s)	1.65 (m)
	$^{11}B\{^1H\}$ NMR, 25 °C	
$M(BH_4)$	−24.0 (s, fwhm = 49)	−26.1 (s, fwhm = 42)
	^{11}B NMR, 25 °C	
$M(BH_4)$	−24.0 (quintet, J_{BH} = 83)	−26.1 (quintet, J_{BH} = 83)
	$^{31}P\{^1H\}$ NMR, 25 °C	
MP	15.3 (m)[d]	12.4 (m)[e]
MP	3.5 (m)[d]	2.5 (m)[e]
	^{31}P NMR, 25 °C	
MP	15.3 ("t", "J_{PH}" = 80)	12.4 ("t", "J_{PH}" = 70)
MP	3.5 (br s)	2.5 (br s)

[a] Coupling constants and line widths (fwhm) in Hertz. [b] X part of AA'BB'XX' spin system with $J_{AA'}$ = 67.6, $J_{BB'}$ = 26.7, $J_{XX'}$ = 5, J_{AB} = 32.7, $J_{AB'}$ = −5.0, J_{AX} = 43, $J_{A'X}$ = 8, J_{BX} = 82, and $J_{B'X}$ = 79. [c] X part of AA'BB'XX' spin system with $J_{AA'}$ = 66.8, $J_{BB'}$ = 17.7, $J_{XX'}$ = 5, J_{AB} = 33.3, $J_{AB'}$ = −19.1, J_{AX} = 41, $J_{A'X}$ = 3, J_{BX} = 73, and $J_{B'X}$ = 64. [d] AA'BB' spin system with $J_{AA'}$ = 67.6, $J_{BB'}$ = 26.7, J_{AB} = 32.7, and $J_{AB'}$ = −5.0. [e] AA'BB' spin system with $J_{AA'}$ = 66.8, $J_{BB'}$ = 17.7, J_{AB} = 33.3, and $J_{AB'}$ = −19.1.

and **2** contain only bridging hydrides (see below).

The $^{11}B\{^1H\}$ NMR spectra of **1** and **2** at 0 °C exhibit two broad peaks of relative intensity 3:2 (Figure 3). Both signals become binomial quintets in the ^1H-coupled spectrum. The $^{31}P\{^1H\}$ NMR spectrum at 0 °C is a singlet, and the proton-coupled ^{31}P NMR spectrum consists of a broad singlet. As the temperature is lowered from 0 to −80 °C, the $^{11}B\{^1H\}$ NMR peaks broaden due to quadrupolar relaxation, while the $^{31}P\{^1H\}$ NMR resonance remains sharp.

It is difficult to assign unambiguously a structure for complexes **1** and **2** based on NMR data alone, although the small magnitude of the $^2J_{PH}$ coupling constant suggests a structure in which the three hydride ligands bridge between the two metals. The odd number of BH_4^- groups requires an asymmetric distribution of ligands among the two metal centers. In order to assign the exact

Table II. ^1H NMR Chemical Shifts of Ti^{IV}, Zr^{IV}, and Hf^{IV} Polyhydrides[a]

compd	δ_t	δ_b	ref
$Cp^*_2TiH_2$	0.28		11
$Zr_2H_3(BH_4)_5PMe_3)_2$		3.96	this work
$ZrH(BH_4)_3$(dmpe)	6.08		this work
$ZrH_2(BH_4)_2$(dmpe)$_2$	3.38		this work
$[Cp_2ZrH_2{\cdot}AlMe_3]_2$		−2.92	14
$[Cp'_2ZrH_2]_2$	3.75	−2.98	15
$[(C_5H_4\text{-}i\text{-}Pr)_2ZrH_2]_2$	3.75	−3.07	17
$[(C_5H_4\text{-}t\text{-}Bu)_2ZrH_2]_2$	3.65	−3.17	17
$[Ind_2ZrH_2]_2$	4.59	−1.56	16
$Cp^*_2ZrH_2$	7.46		12
$Cp^*_2ZrH_2(CO)$	1.07		12
$Cp^*_2ZrH_2(PF_3)$	0.55		12
$[Cp^*ZrH_2(BH_4)]_2$	3.91	1.31	18
$Cp^*_2Zr_2H_3Cl_3(PMe_3)$		4.73, 4.44, 2.97	19
$Hf_2H_3(BH_4)_5(PMe_3)_2$		8.53	this work
$HfH(BH_4)_3$(dmpe)	10.99		this work
$HfH_2(BH_4)_2$(dmpe)$_2$	6.65		this work
$Hf_2H_3(BH_4)_3$(npp)$_2$		8.68	21
$Hf_2H_4(BH_4)_2$(npp)$_2$		9.65	21
$[Cp^*HfH_2Cl]_4$		11.14, 8.44	20
$[(C_5H_4\text{-}i\text{-}Pr)_2HfH_2]_2$	9.54	1.14	17
$[(C_5H_4\text{-}t\text{-}Bu)_2HfH_2]_2$	9.45	1.25	17
$Cp^*_2HfH_2$	15.57		13
$Cp^*_2HfH_2(CO)$	2.67		13

[a] δ_t = chemical shift of terminal hydride, δ_b = chemical shift of bridging hydride, Cp = C_5H_5, Cp' = C_5H_4Me, Cp* = C_5Me_5, Ind = C_9H_7, and npp = $N(SiMe_2CH_2PMe_2)_2$.

Table III. Crystallographic Data for $Zr_2H_3(BH_4)_5(PMe_3)_2$ (**1**) and $Hf_2H_3(BH_4)_5(PMe_3)_2$ (**2**)

	1	2
space group	$P2_12_12_1$	$P2_12_12_1$
T, °C	−75	−75
a, Å	10.921 (2)	10.860 (7)
b, Å	12.255 (3)	12.248 (7)
c, Å	16.524 (6)	16.490 (4)
V, Å	2212 (1)	2193 (3)
Z	4	4
molec wt	411.83	584.36
d_{calcd}, g cm^{-1}	1.236	1.770
μ_{calcd}, cm^{-1}	10.50	95.04
size, mm	0.3 × 0.3 × 0.3	0.2 × 0.2 × 0.2
diffractometer	Enraf-Nonius CAD4	
radiation	Mo K$\bar{\alpha}$, $\bar{\lambda}$ = 0.17073 Å	
monochromator	graphite crystal, 2θ = 12°	
scan range, type	$2.0 \le 2\theta \le 60.0°$, ω/θ	
scan speed, width	3–16 deg/min^{-1}, $\Delta\omega = 1.50[1.00 + 0.35 \tan\theta]°$	
rflctns, total	3827	1923
rflctns, unique	3615	1757
rflctns, $I > 2.58\sigma(I)$	2821	1634
R_I	0.018	0.025
R_F	0.031	0.042
R_{wF}	0.029	0.051
variables	301	112
p factors	0.010	0.010

structures of these dinuclear complexes, we have determined the molecular structures of **1** and **2** by single-crystal X-ray diffraction.

Crystal Structures of 1 and 2. Single crystals of **1** and **2** were obtained by cooling saturated pentane solutions to −20 °C. Crystal data are given in Table III, while selected bond distances and angles are collected in Tables IV and V. Crystals of **1** and **2** are isomorphous, and the asymmetric unit contains one dinuclear molecule that lacks any crystallographically imposed symmetry (Figure 4); the structure of the zirconium complex **1** will be considered first.

Molecules of **1** consist of two zirconium centers that are connected by three bridging hydride ligands. The Zr···Zr contact distance of 3.124 (1) Å is considerably shorter than the Zr···Zr distance of 3.460 (1) Å in the doubly hydride bridged dimer $[Cp'_2ZrH_2]_2$[15] but is comparable to the 3.126 (1) Å Zr···Zr distance in $Cp^*_2Zr_2H_3Cl_3(PMe_3)$.[19] In fact, the Zr···Zr contact in

Table IV. Selected Bond Distances (Å) and Angles (deg) for the Non-hydrogen Atoms in $Zr_2H_3(BH_4)_5(PMe_3)_2$ (**1**) and $Hf_2H_3(BH_4)_5(PMe_3)_2$ (**2**)

	1: M = Zr	2: M = Hf
	Bond Distances	
M1···M2	3.124 (1)	3.076 (1)
-P1	2.750 (1)	2.725 (6)
-P2	2.750 (1)	2.724 (6)
-B1	2.336 (7)	2.33 (2)
-B2	2.604 (8)	2.53 (3)
M2-B3	2.361 (8)	2.34 (3)
-B4	2.332 (7)	2.35 (3)
-B5	2.357 (8)	2.32 (3)
	Bond Angles	
P1-M1-P1	155.06 (4)	154.8 (2)
B1-M1-B2	118.9 (3)	117.8 (9)
B3-M2-B4	106.5 (2)	105.9 (9)
-B5	107.3 (3)	104 (1)
B4-M2-B5	106.2 (3)	106 (1)
M2-M1-P1	97.46 (3)	97.8 (1)
-P2	96.52 (3)	97.6 (1)
-B1	116.1 (2)	115.9 (6)
-B2	124.9 (2)	126.3 (6)
M1-M2-B3	112.6 (2)	114.9 (7)
-B4	112.4 (2)	113.7 (6)
-B5	111.5 (2)	111.4 (7)

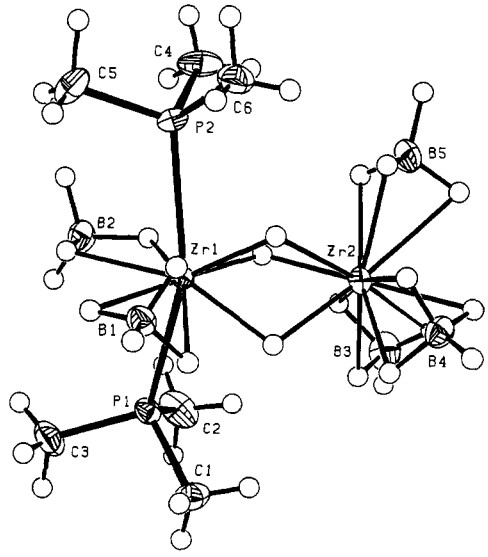

Figure 4. ORTEP diagram of the molecular structure of $Zr_2H_3(BH_4)_5(PMe_3)_2$ (**1**) showing the 35% probability surfaces. The hydrogen atoms are represented by arbitrarily sized spheres.

1 is comparable with the Zr–Zr single bond lengths of 3.104 (2) to 3.182 (1) Å in the Zr^{III} dimers $Zr_2Cl_6(PR_3)_4$.[38,39] As is often the case, metal–metal contact distances cannot be used as a reliable guide to bond order. In the present situation, the bonding constraints of the three bridging hydride ligands undoubtedly are responsible for the short Zr···Zr distance.

The dinuclear unit is remarkably asymmetric: One zirconium center is ligated by three tridentate BH_4^- groups, while the other is coordinated to the two PMe_3 ligands and one bidentate and one tridentate BH_4^- group. Evidently, the hapticity of the BH_4^- ligands is dictated by steric effects; the more crowded zirconium center possesses the only bidentate BH_4^- group in the molecule. The hapticity of the tetrahydroborate ligands is clearly revealed by the Zr···B distances,[40] which are ca. 2.35 and 2.60 Å for the η^3- and η^2-BH_4 groups, respectively. The ligation mode was confirmed in every case by the locations of the hydrogen atoms, which

Table V. Selected Bond Distances (Å) and Angles (deg) for the Hydrogen Atoms in $Zr_2H_3(BH_4)_5(PMe_3)_2$ (**1**)

	Bond Distances		
Zr1-Ha	1.93 (4)	B1-HB1a	1.27 (6)
-Hb	1.84 (7)	-HB1b	1.05 (7)
-Hc	1.83 (6)	-HB1c	1.05 (6)
Zr2-Ha	1.95 (4)	-HB1d	1.11 (5)
-Hb	2.10 (7)	B2-HB2a	1.18 (5)
-Hc	1.86 (6)	-HB2b	1.03 (7)
Zr1-HB1a	1.98 (6)	-HB2c	1.11 (5)
-HB1b	2.23 (7)	-HB2d	1.21 (5)
-HB1c	2.02 (6)	B3-HB3a	1.03 (8)
Zr1-HB2a	2.05 (5)	-HB3b	1.23 (6)
-HB2b	2.22 (6)	-HB3c	1.01 (6)
Zr1-HB3a	2.05 (7)	-HB3d	1.02 (6)
-HB3b	2.17 (6)	B4-HB4a	1.11 (5)
-HB3c	2.14 (5)	-HB4b	1.19 (5)
Zr2-HB4a	2.17 (5)	-HB4c	1.00 (5)
-HB4b	2.04 (5)	-HB4d	1.01 (6)
-HB4c	2.21 (5)	B5-HB5a	1.07 (6)
Zr2-HB5a	2.14 (5)	-HB5b	0.97 (6)
-HB5b	2.09 (6)	-HB5c	1.11 (7)
-HB5c	2.36 (7)	-HB5d	1.17 (5)
	Bond Angles		
Zr1-Ha-Zr2	108 (2)	Hb-Zr1-Hc	61 (3)
Zr1-Hb-Zr2	104 (3)	Ha-Zr2-Hb	60 (2)
Zr1-Hc-Zr2	116 (3)	Ha-Zr2-Hc	60 (2)
Ha-Zr1-Hb	65 (2)	Hb-Zr2-Hc	56 (3)
Ha-Zr1-Hc	60 (2)		

appeared in the difference maps and whose locations were refined with independent isotropic thermal parameters. The B–H distances are 1.09 (6) Å for the BH_4^- hydrogen atoms that are bridging to zirconium and 1.10 (6) Å for the BH_4^- hydrogen atoms that are terminal on boron. Thus, the tetrahydroborate groups do not show the expected 0.06–0.10-Å lengthening of the B–H bonds that bridge between boron and the metal center; evidently, the statistical uncertainties in the hydrogen atom positions are comparable with the chemical differences in the bond lengths. Except for this uncertainty in the hydrogen atom positions, the metal–BH_4 interactions in $Zr_2H_3(BH_4)_5(PMe_3)_2$ are similar to those in $Zr(BH_4)_4$[41] and $Hf(BH_4)_4$.[42]

The Zr–P distances of 2.750 (1) Å fall within the 2.68–2.97-Å range observed for other zirconium(IV) trialkylphosphine complexes.[19,38,39,43] The coordination geometry of the phosphine-ligated zirconium center is not easily describable in terms of conventional coordination polyhedra; however, if one considers the BH_4^- groups to occupy one coordination site each and the three bridging hydrides collectively to occupy another coordination site, then Zr(1) may be said to possess a trigonal bipyramidal geometry with the phosphines in the axial sites. A similar formula applied to Zr(2) gives a tetrahedral geometry for this zirconium center. Interestingly, all three BH_4^- groups on Zr(2) are approximately trans to one of the three bridging hydride ligands. This suggests an alternative view of the coordination geometry about Zr(2), in which the three hydride ligands and the three BH_4^- groups describe a *fac* octahedral coordination sphere.

The Zr–H_b distances to the bridging hydrides range from 1.84 (7) to 2.10 (7) Å and average 1.92 (4) Å. The differences among the individual Zr–H_b distances are not statistically significant, and thus within experimental error the hydrides all bridge symmetrically between the two zirconium centers, despite the asymmetric distribution of BH_4^- and PMe_3 ligands. The 1.92 (4) Å average Zr–H_b distance is shorter than the 2.05 (3) Å value for the bridging hydrides in $[Cp'_2ZrH_2]_2$[15] and the 2.09-Å average in $Cp^*_2Zr_2H_3Cl_3(PMe_3)$,[19] although the difference is only 3 or 4 standard deviations. For comparison, the terminal Zr–H_t distance in $[Cp'_2ZrH_2]_2$ is 1.78 (2) Å, which is similar to the

(38) Wengrovius, J. H.; Schrock, R. R.; Day, C. D. *Inorg. Chem.* **1981**, *20*, 1844–1849.
(39) Cotton, F. A.; Diebold, M. P.; Kibala, P. A. *Inorg. Chem.* **1988**, *27*, 799–804.
(40) Edelstein, N. *Inorg. Chem.* **1981**, *20*, 297–299.
(41) Plato, V.; Hedberg, K. *Inorg. Chem.* **1971**, *10*, 590–594.
(42) Broach, R. W.; Chuang, I-S.; Marks, T. J.; Williams, J. W. *Inorg. Chem.* **1983**, *22*, 1081–1084.
(43) Fryzuk, M. D.; Haddad, T. S.; Berg, D. J. *Coord. Chem. Rev.*, in press.

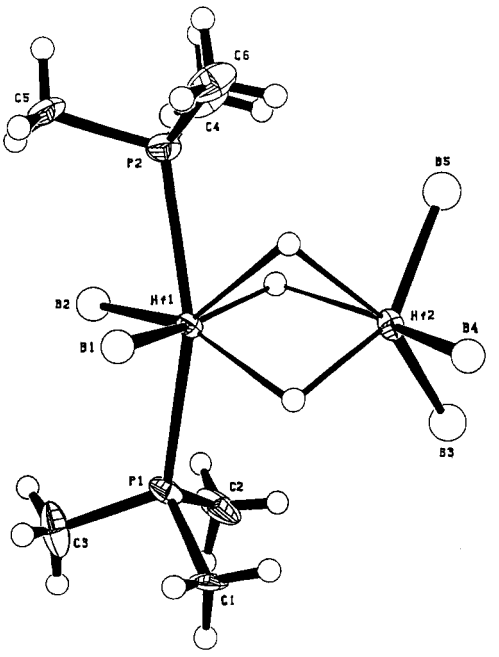

Figure 5. ORTEP diagram of the molecular structure of $Hf_2H_3(BH_4)_5(PMe_3)_2$ (**2**) showing the 35% probability surfaces. The bridging hydrides were not located but are placed in positions analogous to those in the zirconium analogue.

terminal Zr–H distances of 1.67 Å and 1.80 (5) Å in $(\eta^5\text{-}C_8H_{11})ZrH(dmpe)_2$[44] and $CpZrH(C_4H_8)(PMe_3)$,[45] respectively. To our knowledge, only one other bridging zirconium hydride has been crystallographically located, and the hydride atom in $Cp_3ZrH(AlEt_3)$,[46,47] which bridges between Zr and Al, is 1.88 Å from zirconium.

The $Zr\text{–}H_b\text{–}Zr$ angles in **1** of 110(3)° are more acute than the $Zr\text{–}H_b\text{–}Zr$ angle of 120 (1)° in $[Cp'_2ZrH_2]_2$,[15] and this difference, along with the slightly shorter $Zr\text{–}H_b$ distance in **1**, accounts for the disparate Zr···Zr separations in the two molecules. The $H_b\text{–}Zr\text{–}H_b$ angles average 60 (2)°, and this value is identical with the $H_b\text{–}Zr\text{–}H_b$ angle in $[Cp'_2ZrH_2]_2$. The nature of the zirconium–hydride interaction and comparisons with other dinuclear polyhydrides have been discussed previously.[15] The unusually obtuse $M\text{–}H_b\text{–}M$ angles are typical of hydrides that bridge two metals that are not connected by a metal–metal bond. Evidently, the steric repulsion between the methylcyclopentadienyl ligands in $[Cp'_2ZrH_2]_2$ causes the Zr···Zr separation to lengthen and the $Zr\text{–}H_b\text{–}Zr$ angles to become even more obtuse, in comparison with the apparently less crowded molecule **1**.

The molecular structure of the hafnium analogue **2** (Figure 5) is very similar to that of the zirconium analogue, except that the metal–ligand distances are all shorter by 0.02–0.07 Å. Similarly, the Hf···Hf separation of 3.076 (1) Å is 0.048 Å shorter than the Zr···Zr separation in **1**. Unfortunately, the large scattering of Mo X-rays by hafnium prevented the hydrogen atoms from being located.

Fryzuk has previously reported that treatment of the hafnium tetrahydroborate complex $Hf(BH_4)_3(npp)$, (npp = $N(SiMe_2CH_2PMe_2)_2$) with PMe_3 yields a dimeric polyhydride $Hf_2H_3(BH_4)_3(npp)_2$.[21] The ^1H NMR chemical shift of the hydride ligands in this complex of δ 8.68 is very similar to the δ 8.53 shift in **2**. The metal centers in $Hf_2H_3(BH_4)_3(npp)_2$ are separated by 3.143 (1) Å and are connected by three bridging hydrides; furthermore, the coordination environments about the two hafnium

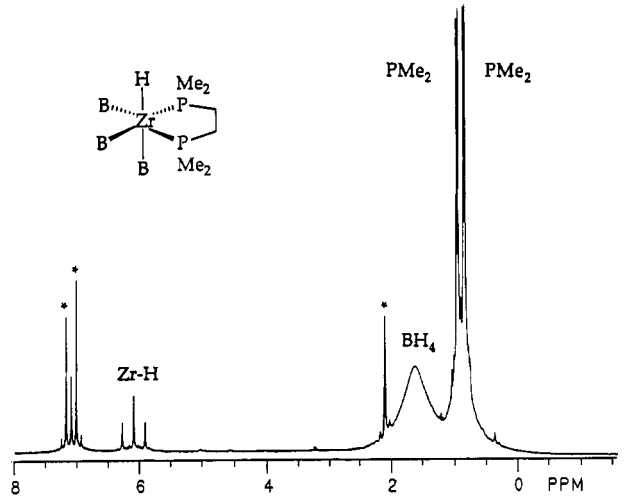

Figure 6. 500-MHz ^1H NMR spectrum of $ZrH(BH_4)_3(dmpe)$ (**3**) at −80 °C in C_7D_8. Solvent peaks are indicated with an asterisk.

atoms are distinctly different. The $Hf\text{–}H_b$ distances average 1.90 (6) Å, and the $Hf\text{–}H_b\text{–}Hf$ angles average 112 (3)°. In these respects, the structures of **1**, **2**, and $Hf_2H_3(BH_4)_3(npp)_2$ are remarkably similar.

Dynamic Behavior of the $M_2H_3(BH_4)_5(PMe_3)_2$ Complexes. The variable-temperature NMR spectra of $Zr_2H_3(BH_4)_5(PMe_3)_2$ and $Hf_2H_3(BH_4)_5(PMe_3)_2$ showed no direct evidence of dynamic behavior. However, the asymmetric structures of these complexes are only consistent with the simplicity of the NMR spectra if dynamic processes are occurring. Specifically, there must be an exchange process that interconverts the $\eta^2\text{-}BH_4^-$ and $\eta^3\text{-}BH_4^-$ groups on Zr(1), since these two ligands are chemically equivalent in the ^1H and ^{11}B NMR spectra. A second exchange process is necessary to interconvert the three tridentate BH_4^- groups on Zr(2), since these are chemically inequivalent in the static structure. Finally, an exchange process is also necessary to interconvert the three bridging hydrides. A rotational motion of the $H_3Zr(BH_4)_3$ group about the Zr(1)···Zr(2) axis would be sufficient to exchange the three bridging hydrides and the three $\eta^3\text{-}BH_4$ groups on Zr(2). Such rotations have been studied theoretically[48] and have been invoked to explain the dynamic NMR behavior of early-transition-metal compounds that contain bridging hydrides, such as $Ta_2H_2Cl_4(PMe_3)_4$[49] and $Hf_2H_3(BH_4)_3(npp)_2$.[21]

Interestingly, the BH_4^- groups on Zr(1) and Zr(2) do not exchange with each other. Although Fryzuk has previously suggested that BH_4^- groups can transfer intramolecularly from one hafnium center to the other in the triply hydrogen bridged compound $Hf_2H_3(BH_4)_3(npp)_2$,[21] we see no evidence of such a process in **1** or **2**.

Reactions of $M(BH_4)_4$ with Bidentate Phosphines. Treatment of the zirconium and hafnium tetrahydroborates $M(BH_4)_4$ with 1 equiv of the bidentate phosphine 1,2-bis(dimethylphosphino)-ethane (dmpe) gives the new monohydride complexes $MH(BH_4)_3(dmpe)$.

$$M(BH_4)_4 + dmpe \rightarrow MH(BH_4)_3(dmpe) + BH_3$$
3: M = Zr
4: M = Hf

The infrared spectra of these complexes clearly reveal the presence of bidentate BH_4^- groups and strongly suggest that at least one tridentate BH_4^- group is present as well. No M–H hydride stretches are apparent; presumably these are obscured by the C–H and B–H bending modes near 1500 cm^{-1}. In other terminal hydride derivatives of zirconium, the Zr–H stretching frequencies occur in the 1540–1650-cm^{-1} region and are often obscured by other bands.

(44) Fischer, M. B.; James, E. J.; McNeese, T. J.; Nyburg, S. C.; Posin, B.; Wong-Ng, W.; Wreford, S. S. *J. Am. Chem. Soc.* **1980**, *102*, 4941–4947.
(45) Wielstra, Y.; Meetsma, A.; Gambarotta, S. *Organometallics*, **1989**, *8*, 258–259.
(46) Senn, H.; Kaminsky, W.; Vollmer, H.-J.; Woldt, R. *Angew Chem., Int. Ed. Engl.* **1980**, *19*, 390–392.
(47) Kopf, J.; Vollmer, H.-J.; Kaminsky, W. *Cryst. Struct. Commun.* **1980**, *9*, 985–990.
(48) Dedieu, A.; Albright, T. A.; Hoffmann, R. *J. Am. Chem. Soc.* **1979**, *101*, 3141–3151.
(49) Wilson, R. B.; Sattelberger, A. P.; Huffman, J. C. *J. Am. Chem. Soc.* **1982**, *104*, 858–860.

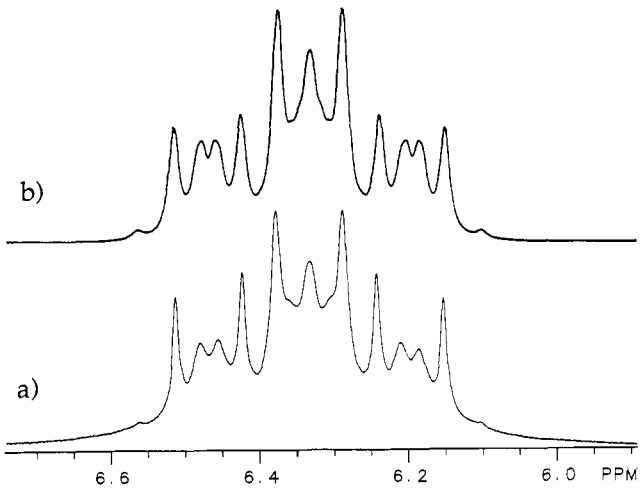

Figure 7. 500-MHz ^1H NMR spectrum of $HfH_2(BH_4)_2(dmpe)_2$ (**6**) at 20 °C in C_7D_8 (only hydride region is shown): (a) observed; (b) computer simulated (see text).

The ^1H NMR spectra of **3** and **4** contain triplets for the ZrH and HfH groups at δ 6.09 and 11.00, respectively (Figure 6). The P–H couplings with the metal-bound hydrides of 55 Hz for **3** and 44 Hz for **4** are remarkably large compared with the 13 Hz J_{PH} coupling constants observed for the bridging hydrides in **1** and **2**; this suggests that the hydride ligands in **3** and **4** are terminal. The ^{11}B and ^{31}P NMR spectra of the $MH(BH_4)_3(dmpe)$ complexes indicate that there is only one BH_4^- environment and one phosphorus environment. However, the ^1H NMR spectrum clearly shows that there are *two* environments for the PMe_2 groups of the dmpe ligands.

The NMR spectra are temperature independent between −80 and +60 °C, except for broadening of the ^1H and ^{11}B NMR resonances of the BH_4^- groups due to quadrupolar effects. Based on these observations, we propose a pseudooctahedral structure for **3** and **4**, where for convenience the BH_4^- groups are each considered to occupy one coordination site. Given a facial arrangement of the ligands (see Figure 6), the NMR data can be understood provided that the chemically inequivalent BH_4^- groups accidentally have the same chemical shifts or are undergoing an exchange process that does not render the diastereotopic PMe_2 groups equivalent. One possibility is that the three mutually facial BH_4^- groups undergo a cyclic permutation; this process would maintain the inequivalence of the PMe_2 groups.

Treatment of the zirconium and hafnium tetrahydroborates with excess dmpe yields new polyhydrides of stoichiometry $MH_2(BH_4)_2(dmpe)_2$. The infrared spectra of these two compounds suggest that all of the BH_4^- groups are bidentate, although there are more bands in the B–H stretching region than are commonly seen for complexes with bidentate BH_4^- groups. No M–H hydride

$$M(BH_4)_4 + 4dmpe \rightarrow MH_2(BH_4)_2(dmpe)_2 + 2BH_3{\cdot}dmpe$$
$$\mathbf{5}: M = Zr$$
$$\mathbf{6}: M = Hf$$

stretches were apparent since these vibrations are probably obscured by the C–H and B–H bending modes.

The corresponding deuterated complex $ZrD_2(BD_4)_2(dmpe)_2$ was prepared by addition of dmpe to $Zr(BD_4)_4$. The infrared spectrum of this selectively deuterated complex shows strong B–D stretches at 1787 and 1733 cm^{-1}, which are shifted some 600 cm^{-1} to lower energy from the corresponding frequencies of the protio analogue. We were unable to identify which infrared bands are due to Zr–D stretching modes since it was not possible to distinguish between these modes and B–D bending and wagging modes that also occur in the 500–1500-cm^{-1} region. The deuterated complex contains some residual B–H bonds as shown by the weak B–H stretching absorptions at 2340 and 2273 cm^{-1}.

Low-Temperature NMR Spectra of the $MH_2(BH_4)_2(dmpe)_2$ Complexes. The ^1H NMR spectra of **5** and **6** each show the presence of four dmpe PMe_2 environments, one BH_4^- environment, and one hydride environment. The hydride resonance consists of a complex multiplet (Figure 7) at δ 3.38 (Zr) or 6.65 (Hf). The $^{11}B\{^1H\}$ NMR spectra confirm that there is only one BH_4^- environment. The $^{31}P\{^1H\}$ NMR spectra of **5** and **6** reveal that the two ends of the dmpe ligands are inequivalent since two equal-intensity resonances are seen. The second-order line shapes seen for each resonance (Figures 8 and 9) reveal that the $^{31}P\{^1H\}$ NMR spectrum is that of an AA′BB′ spin system. Simulation of the patterns for compounds **5** and **6** gives the J_{PP} coupling constants listed in Table I. In general, the zirconium and the hafnium dihydrides have quite similar phosphorus–phosphorus coupling constants.

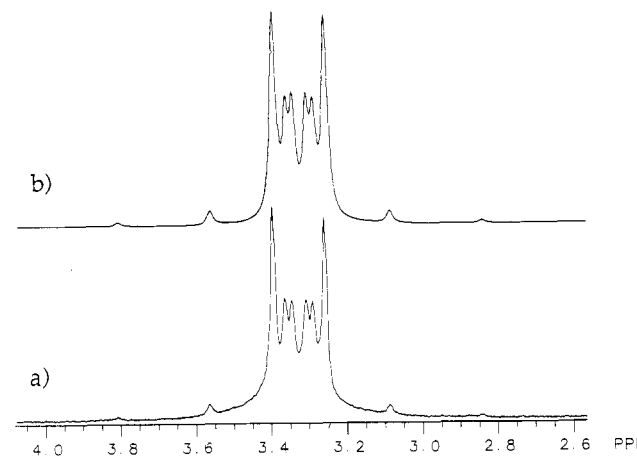

Figure 8. 202-MHz $^{31}P\{^1H\}$ NMR spectrum of $ZrH_2(BH_4)_2(dmpe)_2$ (**5**) at −60 °C in C_7D_8 (only upfield multiplet is shown): (a) observed; (b) computer simulated (see text).

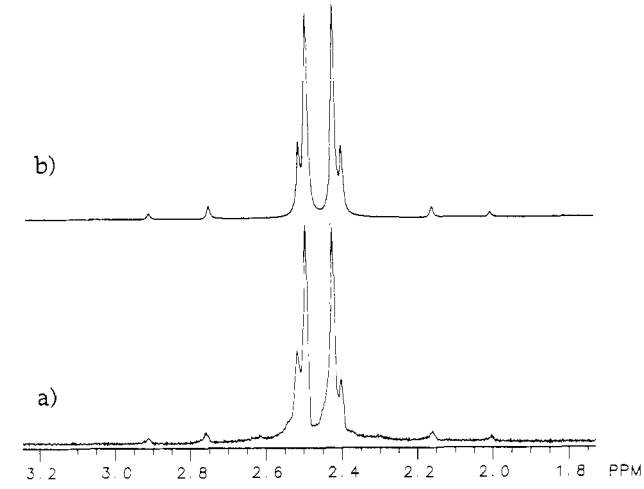

Figure 9. 202-MHz $^{31}P\{^1H\}$ NMR spectrum of $HfH_2(BH_4)_2(dmpe)_2$ (**6**) at −60 °C in C_7D_8 (only upfield multiplet is shown): (a) observed; (b) computer simulated (see text).

The ^1H-coupled ^{31}P NMR spectra of **5** and **6** show that one of the ^{31}P NMR resonances is split into an apparent triplet due to coupling with the two metal-bound hydride ligands. The apparent $^2J_{PH}$ coupling constant is 80 Hz for **5** and 70 Hz for **6**. The other ^{31}P NMR peak is a broad singlet, which indicates that the heteronuclear $^1J_{PH}$ coupling constants between the hydride ligands and these two phosphorus nuclei are small ($\leq$40 Hz).

With this coupling information from the ^{31}P and $^{31}P\{^1H\}$ NMR spectra, the ^1H NMR line shape of the hydride resonances can be interpreted: the pattern is the X part of an AA′BB′XX′ spin system.[50] Of the nine unique coupling constants necessary to describe this spin system, the four that describe the AA′BB′

(50) The hydride ligands are not coupled to the protons of the BH_4^- groups, as shown by a $^1H\{$selective $^1H\}$ NMR decoupling experiment. Although ^{91}Zr and ^{179}Hf are quadrupolar nuclei, their natural abundances are less than 15%, and thus quadrupolar coupling with the hydride ligand is not expected to affect the hydride line shapes significantly.

subspectrum are known. The ^1H NMR spectrum, the proton-coupled ^{31}P NMR spectrum, and several selective-decoupling $^{31}P\{^1H\}$, selective $^{31}P\}$ and $^1H\{$selective $^{31}P\}$ NMR experiments gave reasonably accurate values for J_{AX}, $J_{A'X}$, J_{BX}, and $J_{B'X}$. The ninth coupling constant $J_{XX'}$ is expected to be small based on the homonuclear $^2J_{HH}$ couplings typical of transition-metal polyhydrides.[15] Given these estimates, we were able to simulate the ^1H NMR line shapes (Figure 7). The following conclusions for the zirconium complex **5** also pertain to the hafnium analogue **6**. The optimized values of $J_{AX} = 43$, $J_{A'X} = 8$, $J_{BX} = 82$, and $J_{B'X} = 79$ Hz are accurate to within ca. 5 Hz. However, the spectrum is only weakly dependent on the magnitude of the homonuclear ^1H coupling constant $J_{XX'}$; values between 5 and 30 Hz gave "acceptable" simulations. The uncertainties in the $^2J_{HH}$ and $^2J_{HP}$ coupling constants arise from the presence of numerous closely spaced NMR transitions in the ^1H NMR spectrum, which make it difficult to correlate observed peak positions with specific transitions between calculated energy levels.

Interestingly, the line shapes could best be simulated if the $^2J_{HH}$ coupling constants were about 30 Hz. These coupling constants are considerably larger than the <10 Hz values typical of transition-metal polyhydrides.[15] The d^0 zirconium and hafnium complexes are unlikely to exhibit nonclassical "molecular dihydrogen" structures, which is one principal cause of large $^2J_{HH}$ coupling constants.[51] Instead, we considered the possibility that nuclear exchange phenomena such as those recently discovered in the iridium trihydrides $(CpIrH_3(PR_3)^+$ were also operative here.[52,53] Nuclear exchange processes are possible in these zirconium and hafnium polyhydride complexes since the H–Zr–H bending modes are low in energy (certainly the Zr–H stretching modes are low in energy since they must be below 1450 cm^{-1} in the IR spectra).

Proof of the presence of nuclear exchange processes in transition-metal polyhydrides can often be obtained from examination of the ^1H NMR spectrum of partially deuterated analogues. The deuterated compound $ZrD_2(BD_4)_2(dmpe)_2$ contains residual ZrH groups as shown by a weak resonance at δ 3.15 in the ^1H NMR spectrum. Integration of this resonance and comparison with the intensities of the dmpe peaks reveal that the ZrH/ZrD ratio is about 1:3. If we assume that the proton and deuterium atoms are distributed statistically at the hydride site, then the sample contains approximately 55, 38, and 7% of the ZrD_2, ZrHD, and ZrH_2 isotopomers, respectively.

The ^1H NMR line shape of the residual ZrH groups in this mixture of isotopomers is very similar to that observed for undeuterated samples. Since the ZrHD isotopomer should dominate the ^1H NMR spectrum of the deuterated sample, we conclude that the $^2J_{HH}$ coupling constant must be small, i.e., nearer 5 than 30 Hz. Thus, the results suggest that nuclear exchange processes are not operative in these zirconium and hafnium polyhydrides.

Dynamic NMR Behavior of the $MH_2(BH_4)_2(dmpe)_2$ Complexes. Above 25 °C, the NMR spectra of $ZrH_2(BH_4)_2(dmpe)_2$ and $HfH_2(BH_4)_2(dmpe)_2$ are temperature-dependent. Specifically, the AA'BB' $^{31}P\{^1H\}$ NMR pattern broadens as the temperature is raised, and coalescence occurs at 100 °C at 202.44 MHz. From the variable temperature $^{31}P\{^1H\}$ NMR spectra, an exchange energy (ΔG^*) of 15.6 kcal mol^{-1} can be calculated for both the zirconium and hafnium complexes. Line-shape changes in the ^1H NMR spectra due to this exchange process also are evident as the temperature is raised. Specifically, the hydride resonance collapses, but the central peak and the outermost peaks in the pattern remain sharp (Figure 10). Eventually, the hydride resonance appears as a binomial quintet above 80 °C. These line-shape changes are consistent with a simple fluxional process that exchanges all four ^{31}P nuclei.

If one considers the bidentate BH_4^- groups to occupy one coordination site, then **5** and **6** are pseudo-eight-coordinate. For

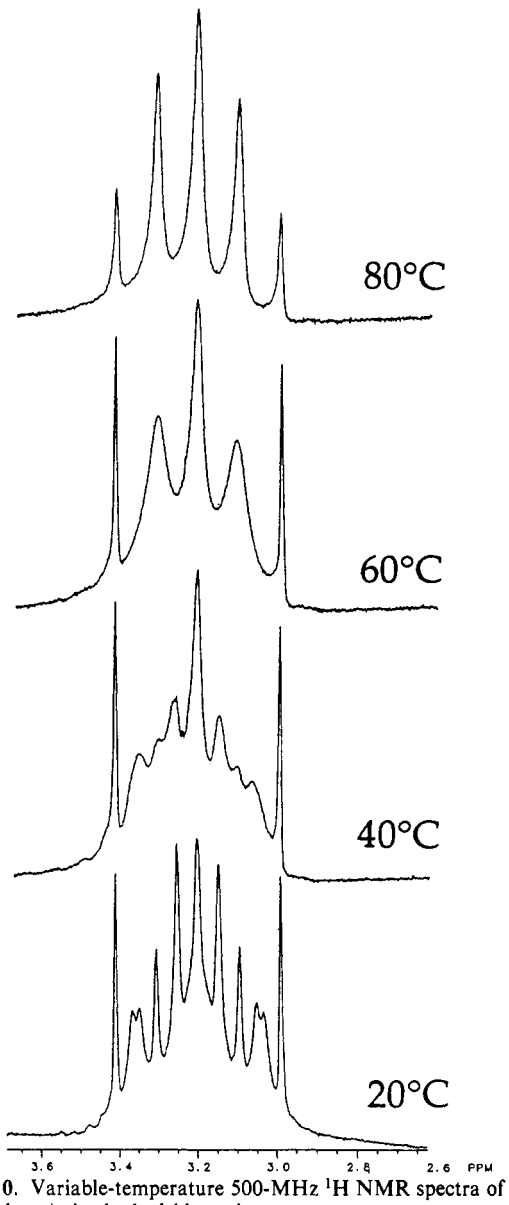

Figure 10. Variable-temperature 500-MHz ^1H NMR spectra of $ZrH_2(BH_4)_2(dmpe)_2$ in the hydride region.

complexes with such high coordination numbers, activation energies of greater than 15 kcal mol^{-1} for fluxional processes are unusually high. A trigonal dodecahedral complex with a similar stoichiometry, $ZrMe_4(dmpe)_2$, has also been reported to be nonfluxional since the ZrMe peak was a second-order multiplet.[54] Evidently, these eight-coordinate $MX_4(dmpe)_2$ species have higher exchange barriers than do other d^0 species; for example, zirconium tetrakis(β-diketonates) have exchange barriers of only 7–8 kcal mol^{-1}.[55] Significantly, the exchange barriers in $ZrH_2(BH_4)_2(dmpe)_2$ and $HfH_2(BH_4)_2(dmpe)_2$ are similar to the 16.5 kcal mol^{-1} barrier of the d^2 complex $WH_4(dppe)_2$, where dppe = 1,2-bis(diphenylphosphino)ethane.[56] The same electronic and steric site preference factors that disfavor fluxional processes in $WH_4(dppe)_2$[56] are probably also operating in the group 4 hydrides. The high barriers for the exchange process may result in part from chemical restrictions on the nature of the fluxional processes. Specifically, the chelating nature of the dmpe ligands will make 16 of the 23 nontrivial permutational isomerisms in $MX_2Y_2(PR_3)_4$ molecules physically impossible. Of the seven chemically allowed nontrivial permutations, one is incompatible with the NMR

(51) Kubas, G. J. *Acc. Chem. Res.* **1988**, *21*, 120–128.
(52) Heinekey, D. M.; Millar, J. M.; Koetzle, T. F.; Payne, N. G.; Zilm, K. W. *J. Am. Chem. Soc.* **1990**, *112*, 909–919.
(53) Zilm, K. W.; Heinekey, D. M.; Millar, J. M.; Payne, N. G.; Neshyba, S. P.; Duchame, J. C.; Szczyrba, J. *J. Am. Chem. Soc.* **1990**, *112*, 920–929.
(54) Girolami, G. S.; Wilkinson, G.; Thornton-Pett, M.; Hursthouse, M. B. *J. Chem. Soc., Dalton Trans.* **1984**, 2789–2794.
(55) Fay, R. C.; Howie, J. K. *J. Am. Chem. Soc.* **1979**, *101*, 1115–1122.
(56) Meakin, P.; Guggenberger, L. J.; Peet, W. G.; Muetterties, E. L.; Jesson, J. P. *J. Am. Chem. Soc.* **1973**, *95*, 1467–1474.

line-shape changes seen above 25 °C. The remaining six permutations fall into four differentiable classes; evidently, none of these permutations corresponds to a low-energy fluxional mechanism.[57]

By analogy with the crystallographically determined structure of $ZrMe_4(dmpe)_2$, we can assume a trigonal dodecahedral arrangement of the ligands in **5** and **6** with the dmpe ligands in the "inner" sites. Accordingly, there are two choices for the relative dispositions of the hydride and tetrahydroborate groups. The two isomers have C_2 symmetry (A) or C_{2v} symmetry (B). However,

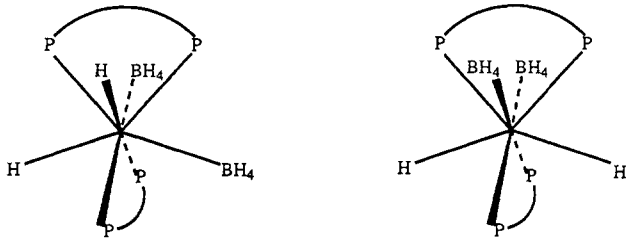

the higher symmetry isomer B would give an A_2B_2 spin system in the $^{31}P\{^1H\}$ NMR spectrum, which is not observed. The C_2 isomer A, however, fits the available data since it gives an AA'BB' spin system for the $^{31}P\{^1H\}$ NMR spectrum and an AA'BB'XX' spectrum for the ^1H NMR resonance of the hydride ligands. Other structures with different coordination geometries are also possible.[58]

Concluding Remarks. We have isolated a series of new polyhydrides of zirconium and hafnium; dinuclear complexes with bridging hydride ligands as well as mononuclear complexes with terminal hydride ligands have been isolated. The molecular structures of the dinuclear species $Zr_2H_3(BH_4)_5(PMe_3)_2$ and $Hf_2H_3(BH_4)_5(PMe_3)_2$ have been determined crystallographically, and the positions of the hydrides were located in the former case. So far, we have been unable to isolate mononuclear zirconium hydrides by treatment of $Zr(BH_4)_4$ with unidentate phosphines.

The dinuclear complexes engage in several dynamic exchange processes that we are unable to freeze out, even at −80 °C. These exchange processes include interconversions between bidentate and tridentate BH_4^- groups, and apparent rotation of a $H_3Zr(BH_3)_3$ unit about the hydride-bridged Zr···Zr vector. In contrast to other polynuclear tetrahydroborates of the group 4 elements, the BH_4^- groups do not exchange between metal centers.

The NMR properties of the mononuclear hydrides are also of interest. For example, the three BH_4^- groups in the monohydrides $ZrH(BH_4)_3(dmpe)$ and $HfH(BH_4)_3(dmpe)$ rapidly exchange between chemically inequivalent sites, while leaving the dmpe PMe_2 methyl groups diastereotopic.

The dihydrides $ZrH_2(BH_4)_2(dmpe)_2$ and $HfH_2(BH_4)_2(dmpe)_2$ are rare examples of 10-coordinate complexes that are nonfluxional at room temperature. In both compounds, the ^1H NMR signals of the hydride ligands are the X part of an AA'BB'XX' spin system. Simulations of the hydride line shapes gave approximate values for the ^{31}P–^{31}P, ^{31}P–^1H, and ^1H–^1H coupling constants. Above 25 °C, these dihydrides are fluxional but the exchange barriers of 15.6 kcal mol^{-1} are unusually high for complexes with such high coordination numbers.

In general, the chemistry of early-transition-metal polyhydrides is still poorly explored. The chemistry of these and other group 4 polyhydrides will be reported separately.

Experimental Section

All operations were carried out in vacuum or under argon. Pentane and diethyl ether were distilled under nitrogen from sodium benzophenone immediately before use. Anhydrous $ZrCl_4$ and $HfCl_4$ were obtained from Cerac and were sublimed under vacuum; $LiBH_4$ (Strem) and $NaBD_4$ (Cambridge Isotopes) were used as received. Trimethylphosphine[59] and 1,2-bis(dimethylphosphino)ethane[60] were prepared by literature routes. Isopropylamine (Aldrich) was dried over KOH and distilled from BaO. Lithium chloride was dried at 185 °C under vacuum.

Despite many attempts, microanalyses of the zirconium and hafnium hydrides were always inaccurate and not reproducible; carbon analyses were usually low by two or more weight percentage units. Sample purity was accordingly established by NMR and IR spectroscopy. The IR spectra were recorded on a Perkin-Elmer 599B infrared spectrometer as Nujol mulls. The ^1H NMR data were obtained on a General Electric QE-300 spectrometer or a General Electric GN-500 spectrometer at 300 or 500 MHz, respectively. The ^{11}B and ^{31}P NMR data were recorded on a GN-300 NB spectrometer at 96.25 and 121.44 MHz, respectively, or on the GN-500 spectrometer at 160.44 and 202.44 MHz. Chemical shifts are reported in δ units (positive shifts to high frequency) relative to $SiMe_4$ (^1H), $BF_3{\cdot}Et_2O$ (^{11}B), or 85% H_3PO_4 (^{31}P). Computer simulations of NMR spectra were performed with the Nicolet software program ITRCAL on a Nicolet 1180E computer.

Tris(μ-hydrido)pentakis(tetrahydroborato)bis(trimethylphosphine)dizirconium(IV) (1). To $ZrCl_4$ (2.00 g, 8.6 mmol) and $LiBH_4$ (0.75 g, 34.4 mmol) was added diethyl ether (40 mL). The white mixture was stirred at 25 °C for 10 min. The volatile material, consisting of solvent and $Zr(BH_4)_4$, was distilled under vacuum from the room temperature reaction flask to a receiver cooled to −196 °C. The distillate was warmed to −78 °C and treated with PMe_3 (2.6 mL, 26 mmol). The resulting mixture was stirred for 1 h at −78 °C and then for 1 h at −10 °C. The solvent was removed at −10 °C to give a light tan solid. The borane adduct $BH_3{\cdot}PMe_3$ was removed at room temperature under vacuum by sublimation onto a cold finger cooled to −78 °C. The nonvolatile residue was extracted with pentane at 0 °C (2 × 40 mL), and the clear red-brown extracts were combined, filtered, concentrated to ca. 55 mL, and cooled to −20 °C to afford amber-colored prisms of the product. Yield: 0.58 g (33%). Mp: 103 °C dec. IR (cm^{-1}): 2550 m, 2505 s, 2435 m, 2390 m, 2220 w, 2155 m, 2102 s, 1520 s br, 1418 m, 1300 w, 1285 m, 1197 s, 1150 w, 1130 s, 1090 sh, 950 s, 842 w, 775 m, 735 m, 730 m, 460 m.

Tris(μ-hydrido)pentakis(tetrahydroborato)bis(trimethylphosphine)dihafnium(IV) (2). This complex was prepared similarly from $HfCl_4$ (4.97 g, 15.5 mmol) and $LiBH_4$ (3.04 g, 140 mmol) in diethyl ether (40 mL), followed by distillation, addition of PMe_3 (4.7 mL, 46.6 mmol), and crystallization from pentane to give colorless prisms. Yield: 2.62 g (29%). Mp: 135 °C dec. IR (cm^{-1}): 2545 m, 2505 s, 2430 m, 2385 m, 2210 w, 2160 w, 2105 s, 1535 s br, 1415 m, 1300 w, 1285 m, 1235 w, 1202 m, 1170 m, 1130 s, 1090 w, 945 s, 838 w, 802 m, 730 m, 722 m, 460 m.

Hydridotris(tetrahydroborato)[1,2-bis(dimethylphosphino)ethane]zirconium(IV) (3). To $ZrCl_4$ (1.01 g, 4.33 mmol) and $LiBH_4$ (0.75 g, 34.4 mmol) was added diethyl ether (40 mL). The white mixture was stirred at 25 °C for 5 min. The volatile components diethyl ether and $Zr(BH_4)_4$ were distilled under vacuum from the room temperature reaction flask to a receiver cooled to −196 °C. The distillate was warmed to −78 °C and treated with dmpe (0.75 mL, 4.50 mmol) to give a milky white mixture. The solution was stirred for 1 h at −78 °C before being warmed to 25 °C. The solution was stirred for 2 h at 25 °C, and then the solvent was removed under vacuum. The resulting solid was washed with pentane (2 × 40 mL), and the residue was extracted with diethyl ether (2 × 40 mL) to give a yellow cloudy solution. The combined extracts were filtered, concentrated to ca. 30 mL, and cooled to −20 °C to afford off-white platelike crystals. Recrystallization from diethyl ether (5 mL) at −20 °C gave a light brown microcrystalline product. Yield: 0.60 g (53%). Mp: 86 °C dec. IR (cm^{-1}): 2510 m, 2475 m, 2365 m, 2180 sh, 2135 m, 2085 sh, 2045 w, 1530 m br, 1420 m, 1305 vw, 1290 m, 1245 m br, 1200 w br, 1160 sh, 1145 sh, 1130 m, 1080 sh, 1065 sh, 1005 vw, 950 s, 940 s, 905 m, 850 m, 805 vw, 775 w, 715 m, 655 w.

Hydridotris(tetrahydroborato)[1,2-bis(dimethylphosphino)ethane]hafnium(IV) (4). This compound was prepared (by following the procedure above for the zirconium analogue) from $HfCl_4$ (1.25 g, 3.90 mmol) and $LiBH_4$ (1.02 g, 46.8 mmol) in diethyl ether (40 mL). After distillation of the $Hf(BH_4)_4$, addition of dmpe (0.65 mL, 3.90 mmol), and crystallization from diethyl ether, off-white blocks were obtained. Yield: 0.45 g (33%). Mp: 198 °C dec. IR (cm^{-1}): 2500 m br, 2360 m br, 2160 s, 2060 m br, 1420 m, 1300 m, 1250 w, 1170 w, 1130 m br, 940 m br, 930 sh, 865 m, 755 m, 705 m, 655 w.

(57) Klemperer, W. G. *Dynamic Nuclear Magnetic Resonance Spectroscopy*; Jackman, L. M., Cotton, F. A., Eds.; Academic Press: New York, 1975; Chapter 2.

(58) The crystal structure of $ZrH_2(BH_4)_2(dmpe)_2$ has been determined by R. T. Baker, F. N. Tebbe, and J. C. Calabrese of DuPont; the zirconium center does in fact adopt a trigonal dodecahedral geometry as shown in structure A. We thank Dr. Baker for sharing their results with us.

(59) Luetkens, M. L.; Sattelberger, A. P.; Murray, H. H.; Basil, J. D.; Fackler, J. P. *Inorg. Synth.* **1989**, *26*, 7–12.

(60) Henderson, R. A.; Hussain, W.; Leigh, G. J.; Normanton, F. B. *Inorg. Synth.* **1985**, *23*, 141–143.

Dihydridobis(tetrahydroborato)bis[1,2-bis(dimethylphosphino)ethane]zirconium(IV) (5). To $ZrCl_4$ (1.10 g, 4.7 mmol) and $LiBH_4$ (0.98 g, 45.6 mmol) was added diethyl ether (40 mL). The white mixture was stirred at 25 °C for 10 min. The volatile material, consisting of solvent and $Zr(BH_4)_4$, was distilled under vacuum from the room temperature reaction flask to a receiver cooled to −196 °C. The distillate was warmed to −78 °C and treated with dmpe (3.2 mL, 19.0 mmol). The resulting mixture was warmed to 0 °C, stirred for 1 h, and then stirred at 25 °C for 45 min. The volatile material was removed under vacuum, and the white solid was washed with pentane (2 × 20 mL) to remove the phosphine–borane byproduct. Yield: 1.50 g (75%). Mp: 141–142 °C. IR (cm^{-1}): 2370 s, 2320 s, 2210 m, 2180 m, 2155 s, 2110 s, 2015 w, 1465 s, 1420 s, 1342 w, 1295 m, 1280 m, 12009 w, 1185 m, 1115 s, 1065 m, 1020 m, 992 w, 942 s, 927 s, 890 m, 855 m, 837 m, 795 m, 760 m, 733 m, 718 w, 698 m, 640 m, 630 m, 568 w, 435 w.

Lithium Tetradeuterioborate ($LiBD_4$).[61,62] A sample of $NaBD_4$ (9.00 g, 0.215 mol) was dissolved in dry isopropylamine (350 mL), and the solution was filtered to remove insoluble impurities. The clear colorless solution was brought to a gentle reflux and treated with anhydrous lithium chloride (11.4 g, 0.269 mmol). A white precipitate formed immediately, and the solution was heated to reflux for 12 h. The white precipitate formed immediately, and the solution was heated to reflux for 12 h. The white precipitate was collected by filtration and dried in vacuum at 165 °C. The solid was treated with diethyl ether (350 mL), and the slurry was heated to reflux for 1 h. The resulting solution was filtered, and the filtrate was taken to dryness under vacuum to yield a colorless dry solid. Yield: 3.84 g (69%). IR (cm^{-1}): 2365 m, 2285 m, 1867 vw br, 1769 s, 1665 vw, 1655 vw, 1625 vw, 1260 w, 1098 vw br, 1015 vw br, 943 m, 921 m, 830 m, 795 vw br. Anal. Calcd for $LiBD_4 \cdot (0.04)NaBD_4 \cdot (0.02)Et_2O$: C, 3.33; H/D, 29.5; B, 38.9; Li, 24.0; Na, 3.18. Found: C, 3.60; H/D, 29.6; B, 37.1; Li, 24.4; Na, 3.18.

Dideuteriobis(tetradeuterioborato)bis[1,2-bis(dimethylphosphino)ethane]zirconium(IV) (5-d_{10}). This compound was prepared as described for the protio analogue above from $ZrCl_4$ (1.00 g, 4.29 mmol), $LiBD_4$ (0.89 g, 34.3 mmol), and dmpe (2.0 mL, 12.0 mmol). Yield: 1.10 g (54%). IR (cm^{-1}): 2340 w, 2273 vs, 1787 s, 1733 s, 1673 w br, 1614 w br, 1524 w br, 1430 w br, 1420 m, 1296 w, 1281 m, 1213 vw br, 1130 w, 1078 w, 1044 vw br, 1008 w, 944 s, 930 sh, 891 m, 838 m, 783 vw, 733 m, 700 m, 647 w, 629 vw, 523 w, 438 vw.

Dihydrobis(tetrahydroborato)bis[1,2-bis(dimethylphosphino)ethane]hafnium(IV) (6). This complex was prepared from $HfCl_4$ (1.15 g, 3.6 mmol) and $LiBH_4$ (1.01 g, 46.9 mmol) in diethyl ether (40 mL), followed by distillation, addition of dmpe (3.0 mL, 18.0 mmol), and workup as above. Yield: 1.15 g (63%). Mp: 88 °C. IR (cm^{-1}): 2362 s, 2325 s, 2215 m, 2175 m, 2155 s, 2118 s, 2015 w, 1475 s, 1410 s, 1290 m, 1277 m, 1180 m, 1110 s, 1073 w, 1060 m, 1010 m, 1010 m, 987 w, 932 s br, 887 m, 850 w, 832 m, 790 m, 730 s, 695 s, 630 s, 560 w, 430 w.

Crystallographic Studies.[63] Single crystals of $Zr_2H_3(BH_4)_5(PMe_3)_2$, (**1**), grown from pentane, were mounted on glass fibers with Paratone-N oil and immediately cooled to −75 °C in a nitrogen stream on the diffractometer. [Single crystals of the hafnium analogue $Hf_2H_3(BH_4)_5(PMe_3)_2$ (**2**) were also grown from pentane, mounted on glass fibers with Paratone-N oil, and immediately cooled to −75 °C. Subsequent comments in brackets will refer to this compound.] Preliminary photographs yielded rough cell dimensions, and standard peak search and automatic indexing procedures, followed by least-squares refinement with 25 reflections, yielded the cell dimensions given in Table I.

Data were collected in one octant of reciprocal space ($-h, +k, -l$) [($-h, -k, -l$)] by using measurement parameters listed in Table I. Additional data in all eight octants were collected for $2.0 < 2\theta < 9.0°$. Systematic absences for $h00$ ($h \neq 2n$), $0k0$ ($k \neq 2n$), and $00l$ ($l \neq 2n$) were consistent only with space group $P2_12_12_1$. The measured intensities were reduced to structure factor amplitudes and their esd's by correction for background, scan speed, and Lorentz and polarization effects. While corrections for crystal decay were unnecessary, absorption corrections were applied. Systematically absent reflections were deleted, and symmetry equivalent reflections were averaged to yield the set of unique data. Only those data with $I > 2.58\ \sigma(I)$ were used in the least-squares refinement.

The structure of the zirconium complex was solved by starting from the atomic coordinates deduced for the isomorphous hafnium analogue. [The structure of **2** had previously been solved by Patterson (SHELX-86) and weighted and unweighted difference Fourier methods. The positions of the hafnium atoms were deduced from a vector map, and subsequent difference Fourier calculations revealed the positions of the remaining nonhydrogen atoms.] The quantity minimized by the least-squares program was $\Sigma w(|F_o| - |F_c|)_2$, where $w = 1.56/(\sigma(F_o)^2 + (pF_o)^2)$. [For **2**, $w = 1.00/(\sigma(F_o)^2 + (pF_o)^2)$.] The analytical approximations to the scattering factors were used, and all structure factors were corrected for both the real and imaginary components of anomalous dispersion. In the final cycle of least squares, all non-hydrogen atoms were independently refined with anisotropic thermal coefficients. Hydrogen atoms were located in the Fourier difference maps, and their locations were independently refined with isotropic thermal parameters. An empirical isotropic extinction parameter was refined, and converged to 5.6 (6) × 10^{-8}. [For **2**, isotropic thermal coefficients were refined for the boron atoms and anisotropic thermal parameters were refined for the remaining nonhydrogen atoms. Methyl hydrogen atoms were included as fixed contributors in "idealized positions" (staggered with respect to the substituents on the phosphorus atom), and a group isotropic thermal parameter was refined for them. The remaining hydrogen atom positions could not be calculated with certainty.] Successful convergence was indicated by the maximum shift/error of 0.065 [0.019] in the last cycle. Final refinement parameters are given in Table I. The final difference Fourier map had no significant features. [For **2**, the largest peaks in the final difference Fourier map were located in the vicinity of the hafnium atoms.] There were no apparent systematic errors among the final observed and calculated structure factors. [For **2**, a final analysis of variance between observed and calculated structure factors showed a slight inverse dependence on sin θ.]

Acknowledgment. We thank the National Science Foundation (Grant CHE 89-17586) and the Department of Energy (Contract DE-AC 02-76 ER 1198) for support of this research. We thank Dr. James A. Jensen, Dr. Vera Mainz, and Robert Morris of the University of Illinois for their assistance. We particularly thank Dr. Scott Wilson and Charlotte Stern of the University of Illinois X-ray Crystallographic Laboratory for carrying out the crystallographic studies. G.S.G. is the recipient of an A. P. Sloan Research Foundation Fellowship (1988–1990) and a Henry and Camille Dreyfus Teacher-Scholar Award (1988–1993).

Supplementary Material Available: Tables of atomic coordinates for **1** and **2**, thermal parameters for **1** and **2**, calculated hydrogen atom positions for **2**, and complete bond distances and angles for **1** and **2** (9 pages); listings of final observed and calculated structure factor amplitudes for **1** and **2** (24 pages). Ordering information is given on any current masthead page.

(61) Schlesinger, H. I.; Brown, H. C.; Hyde, E. K. *J. Am. Chem. Soc.* **1953**, *75*, 209–213.
(62) Atkinson, J. G.; MacDonald, D. W.; Stuart, R. S.; Tremaine, P. H. *Can. J. Chem.* **1967**, *45*, 2583–2588.
(63) For details of the crystallographic programs and procedures used, see ref 29.